

1 *Communication*

2 **Triglycine-based approach for identifying the** 3 **substrate recognition site of an enzyme**

4 **Ki Hyun Nam**^{1,2,*}

5 ¹ Division of Biotechnology, Korea University, Seoul 02481, Republic of Korea

6 ² Institute of Life Science and Natural Resources, Korea University, Seoul 02481, Republic of Korea

7 * Correspondence: structures@korea.ac.kr; Tel.: 82-10-5208-5730 (N.K.H.)

8

9 **Abstract:** Various peptides or non-structural amino acids are recognized by their specific target
10 proteins and perform biological role in various pathways *in vivo*. Understanding the interactions
11 between target protein and peptides (or non-structural amino acids) provides key information on
12 the molecular interactions, which can be potentially translated to the development of novel drugs.
13 However, it is experimentally challenging to determine the crystal structure of protein-peptide
14 complexes. To obtain structural information on substrate recognition of peptide-recognizing
15 enzyme, X-ray crystallographic studies were performed using triglycine (Gly-Gly-Gly) as main-
16 chain of peptide. The crystal structure of *Parengyodontium album* Proteinase K in complex with
17 triglycine was determined at 1.4 Å resolution. Two different bound conformations of triglycine were
18 observed at the substrate recognition site. The triglycine backbone forms stable interactions with β5-
19 α4 and α5-β6 loops of main-chain. One of the triglycine-binding conformations was identical with
20 the binding mode of a peptide-based inhibitor from a previously reported crystal structure of
21 Proteinase K. Triglycine has potential application X-ray crystallography to identify substrate
22 recognition sites in peptide binding enzymes.

23 **Keywords:** protein-protein interaction, protein-peptide interaction, triglycine, substrate binding site,
24 peptide, inhibitor, Proteinase K
25

26 **1. Introduction**

27 Protein-protein interactions (PPIs) regulate most of the cellular processes such as enzyme
28 activities, intracellular localization and/or physical interactions [1, 2]. PPIs can be broadly classified
29 into two types, protein-protein interactions (between domains of two proteins) and protein-peptide
30 interactions (between a protein and linear sequence of other protein) [3]. In PPIs, proteins recognize
31 the short peptide sequences in either sequence-dependent or -independent manner [4]. Peptides bind
32 to cavities, grooves, or pockets in either the active site or substrate recognition sites on the proteins.
33 Alternately, the peptides interact with the β-strands on the protein surface [4]. Investigation of the
34 PPIs is necessary to understand mechanistic details of biological processes and to develop novel
35 drugs [5-7]. Among the various methods for PPI-based drug development, structure-based approach
36 has been widely employed, as in fragment-based drug discovery (FBDD) [8], to identify potential
37 lead compounds for drug development. Although the initial success is usually lesser than that
38 obtained by high-throughput screening (HTS) techniques, FBDD is considered more efficient in the
39 optimization phase [9, 10].

40 Peptide-based fragments can be used to understand structural and mechanistic features of PPIs
41 and to obtain information on FBDD. I hypothesized that a crystallographic study using triglycine
42 (Gly-Gly-Gly or glycyl-glycyl-glycine) molecules could provide information on the main-chain
43 interactions of PPIs. To demonstrate this hypothesis, proteinase K (EC 3.4.21.64) from fungus
44 *Parengyodontium album* (formerly *Tritirachium album*), named as PaProK, was used as a model in this
45 experiment. This enzyme is a broad-spectrum serine protease and predominantly cleaves the internal

46 peptide bonds adjacent to the carboxyl group of aliphatic and aromatic hydrophobic amino acids [11].
47 The active site consists of a catalytic triad Asp39-His69-Ser224 and the substrate recognition site is
48 formed by Gly100-Tyr104 and Ser132-Gly136, which form a triple antiparallel β -strand with the
49 substrate [12].

50 To investigate the structural features of PPI, here I attempted X-ray crystallographic study using
51 triglycine and determined crystal structure of PaProK-triglycine complex at 1.4 Å resolution. The
52 triglycine was bound in two conformations to the substrate recognition site between β 5- α 4 and α 5- β 6
53 loops in PaProK. The conformations of bound triglycine were compared with previously reported
54 crystal structures of PaProK complexed with a peptide-based inhibitor. This structural investigation
55 of the triglycine-PaProK interaction could provide useful information for understanding PPI.
56

57 2. Materials and Methods

58 2.1. Sample preparation

59 Proteinase K from *Paronyodontium album* was purchased from Geogichem (PR3050).
60 Protein was dissolved and resuspended in 50 mM HEPES-NaOH (pH 7.0), and crystallized at 22 °C
61 using the hanging-drop vapor diffusion method. Crystallization drops were set by mixing 1 μ l of
62 PaProK (30 mg/ml) solution with 1 μ l of a reservoir solution (0.1 M Tris-HCl at pH 8.0 and 2.0 M
63 ammonium sulfate) and incubated with 0.5 ml of reservoir solution. Suitable crystals (0.15 \times 0.10 \times
64 0.10 mm) for X-ray diffraction were obtained within two weeks. For PaProK-triglycine complex
65 crystals, 2 μ l of 0.3 M triglycine solution was added to the crystallization drop and incubated for 30
66 min.

67 2.2. X-ray diffraction and data processing

68 The crystals were transferred to a reservoir buffer containing 25% (v/v) glycerol as
69 cryoprotectant. Diffraction data were collected at 100 K on beamline 11C at the Pohang Light Source
70 II (PLS-II, Pohang, South Korea) using Pilatus 6 M detector [13]. The diffraction data sets were
71 processed and reduced using the HKL2000 program [14]. Data collection statistics are presented in
72 Table 1

73 2.3. Structure determination

74 PaProK structure was solved by the molecular replacement method using MOLREP [15] from
75 the CCP4 program suite [16], with the coordinates from the Proteinase K structure (PDB: 1IC6)[17],
76 as the search model. The manual model building and refinement were performed using COOT [18]
77 and phenix.refinement in PHENIX [19], respectively. Refinement statistics are presented in Table 1.
78 Figures were generated with PyMOL (<http://pymol.org/>). The final structures were validated by the
79 MolProbity [20]. The coordinates and structural factors have been deposited in the Protein Data Bank
80 with an accession code, 6KKF.

81

82 3. Results

83 3.1. Overall structure

84 The crystals of the PaProK - triglycine complex belonged to monoclinic space group P2₁,
85 containing one molecule in the asymmetric unit. The electron density map was clear for the
86 interpretation from Ala106 to Gln383. The final structure of PaProK-triglycine was refined to 1.4 Å
87 resolution with R_{work} and R_{free} values of 18.22% and 21.81%, respectively.
88

89

Table 1. Data collection and refinement statistics.

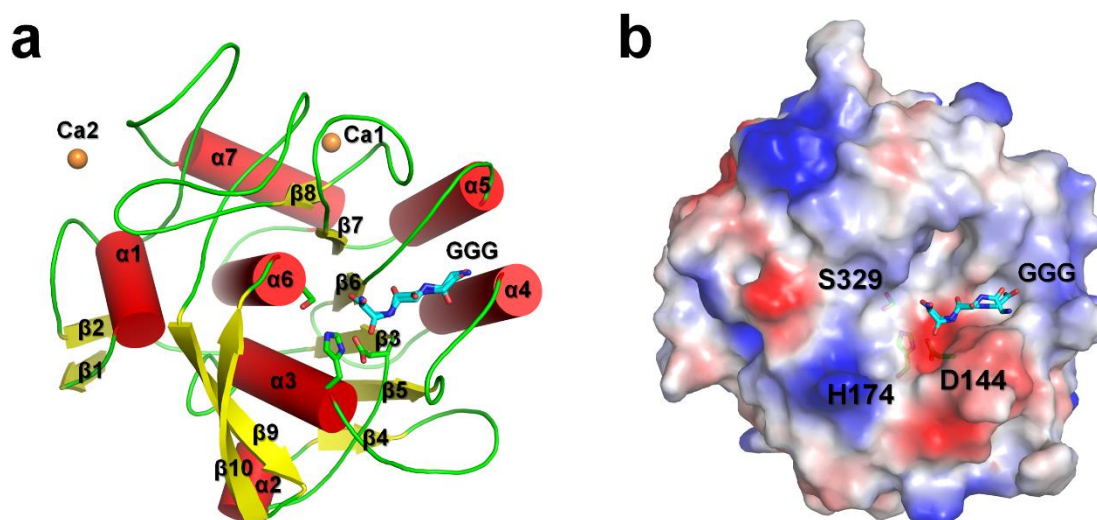
Data collection	PaProK-Triglycine
Resolution	50.0-1.40 (1.42-1.40)
Space group	P2 ₁
Unique reflections	38738 (1831)
Unit cell parameter	
a, b, c (Å)	38.51, 67.68, 43.59
α , β , γ (°)	90.00, 111.39, 90.00
Completeness (%)	94.8 (89.4)
Multiplicity	3.8 (3.7)
<i>I</i> / σ (<i>I</i>)	25.65 (5.17)
R _{merge}	0.166 (0.529)
R _{pim}	0.096 (0.313)
Refinement	
Resolution	40.59-1.40
R _{factor}	18.22
R _{free}	21.81
Average B factor (Å ²)	
protein	11.95
triglycine	19.00
calcium	18.60
water	22.03
R.m.s.deviations	
bonds	0.008
angles	0.993
Ramachandran	
preferred	96.53
allowed	3.09
outliers	0.39

90 Values in the parentheses refer to the highest resolution shell.

91 PaProK displayed a typical $\alpha\beta$ -hydrolase fold with seven α -helices and ten β -strands. The six
 92 central β -strands (β 3- β 8) are surrounded by five peripheral α -helices (α 3- α 7) (Figure 1a). This
 93 structure is similar to the previously reported crystal structures of PaProK (PDB code: 1IC6) [17], with
 94 a Root-Mean-Square Deviation (RMSD) of 0.2892 Å. Ramachandra plot revealed that geometry of
 95 Asp144 on β 3- α 2 loop is ill-defined due to its torsion angles, phi (Φ) and psi (Ψ), at -172° and -142°,
 96 respectively. Asp144 residue is part of the catalytic triad with His222 and Ser329. This ill-defined
 97 geometry of catalytic triad is often observed in the serine proteases or esterase [21-24]. The O δ 1 and
 98 O δ 2 atoms of Asp144 residue (charge-relay) are stabilized by hydrogen bonds with the N δ atom of
 99 His174 (proton carrier), which is at a distance of 2.70 and 3.03 Å, respectively.

100 Electron density map clearly shows that PaProK contains two Ca²⁺ ions (named, Ca1 and Ca2)
 101 (Figure 1A). These Ca²⁺ ions are involved in the thermal stability, but not in the proteolytic activity
 102 [12]. B-factors for the entire protein, Ca1, and Ca2 at 11.89 Å², 7.4 Å² and 28.0 Å², respectively, indicate
 103 that Ca1 binds the protein strongly than Ca2. Ca1 was octahedrally coordinated by carbonyl groups
 104 of Pro280 (2.42 Å) and Val282 (2.39 Å), two carboxylate oxygens Asp305 (2.65 Å and 2.40 Å for O δ 1
 105 and O δ 2, respectively) and four water molecules (2.33-2.51 Å). Ca2 was coordinated by carbonyl
 106 groups of Thr121 (2.49 Å), Asp365 (2.44 Å and 2.36 Å for O δ 1 and O δ 2, respectively) and one water
 107 molecule (2.46 Å). The triglycine is located on the negatively charged substrate binding pocket
 108 around the catalytic triad (Figure 1b).

109



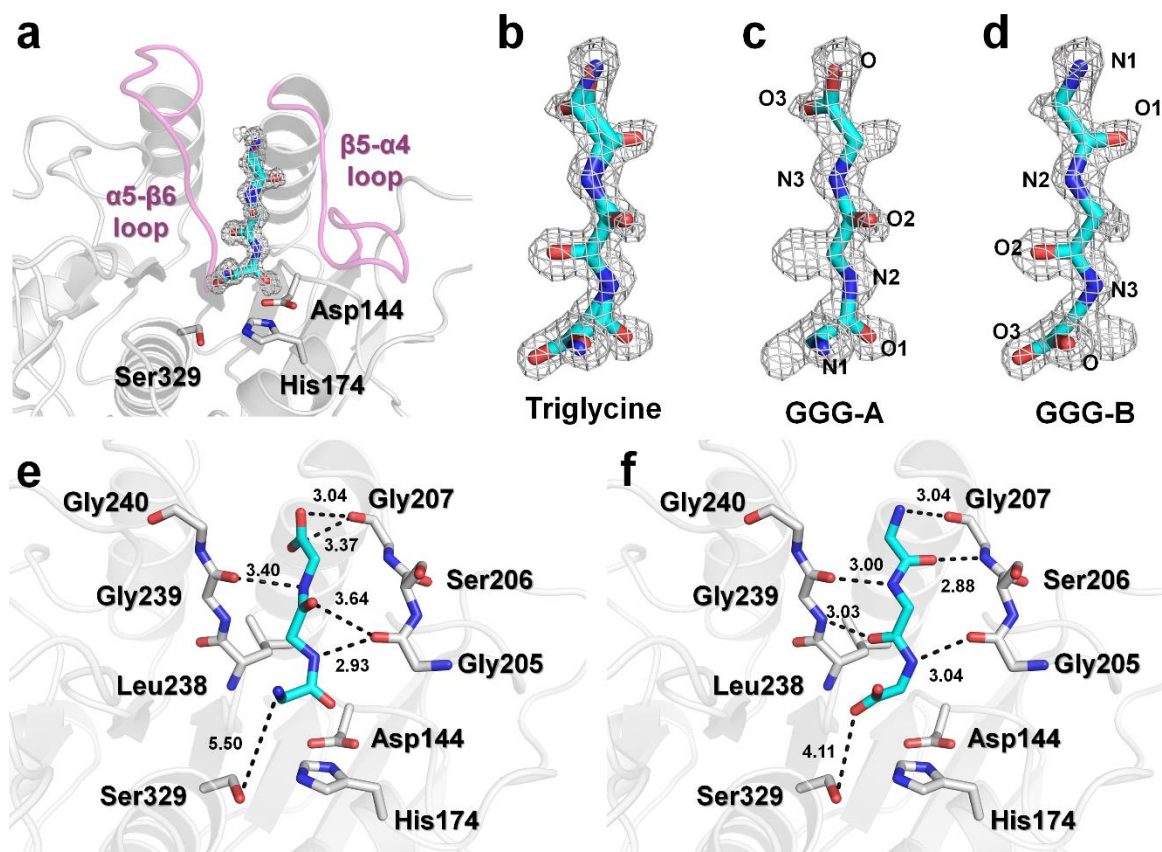
110
 111 **Figure 1.** Crystal structure of PaProK complexed with triglycine (GGG). (a) Cartoon and (b)
 112 electrostatic potential surface representation of Proteinase K. Triglycine (GGG) and Ca ions
 113 are indicated as sticks (cyan) and orange sphere, respectively.

114

115 3.2. Triglycine binding site on PaProK

116 The electron density for triglycine was found at the substrate binding pocket between $\beta 5$ - $\alpha 4$ and
 117 $\alpha 5$ - $\beta 6$ loops around the active site (Figure 2a) [17]. Electron density for the triglycine molecule was
 118 not observed at any other positions, indicating that triglycine can bind only to the peptide
 119 binding site on PaProK. Interestingly, the electron density map of triglycine reveals two binding
 120 conformations, GGG-A and GGG-B (Figure 2b); while the amino-terminus of triglycine is directed
 121 toward PaProK active site in GGG-A (Figure 2c), the carboxy-terminus is directed toward the active
 122 site in GGG-B (Figure 2d). Refinement shows that GGG-A and GGG-B had a 0.56:0.44 ratio of
 123 occupancy on PaProK. The N2, N3, O2, O3 and carboxyl oxygen atoms of the GGG-A interact with
 124 oxygen atoms of Gly205 (2.93 Å), Gly239 (3.40 Å), Gly205 (3.64 Å), Gly207 (3.37 Å) and Gly207 (3.04
 125 Å), respectively (Figure 2e). The N1 atom of triglycine is 5.5 Å away from the hydroxyl group of
 126 Ser329. The N1, O1, N2, O2 and N3 atoms of GGG-B interact with oxygen atom of Gly207 (3.04 Å),
 127 nitrogen atom of Gly207 (2.88 Å), oxygen atom of Gly239 (3.00 Å), nitrogen atom of Gly239 (3.03 Å),
 128 the oxygen atom of Gly207 (3.04 Å), respectively (Figure 2f). The O3 atom of triglycine is 4.2 Å
 129 from the hydroxyl group of Ser329. As a result, the triglycine backbone of both conformations can be
 130 stably maintained by hydrogen bonds on the substrate binding site. In particular, GGG-B forms a
 131 triple antiparallel β -strand with the $\beta 5$ - $\alpha 4$ and $\alpha 5$ - $\beta 6$ loops. While proteins involved in PPI generally
 132 recognize specific amino acid sequences of the substrate, triglycine, due to the lack of side chains, is
 133 considered to bind the substrate binding site with a lower affinity, compared with the general
 134 substrates of PaProK.

135



136

137 **Figure 2.** Binding conformations of triglycine on PaProK. (a-d) 2Fo-Fc electron density of a triglycine
 138 on PaProK (grey colored mesh, 1.5 σ). (a) Triglycine is located between $\beta 5$ - $\alpha 4$ and $\alpha 5$ - $\beta 6$ loops (pink).
 139 (b) Electron density maps reveal two conformations of triglycine. (c) GGG-A and (d) GGG-B forms of
 140 triglycine molecules fitted into the electron density map. Interactions between PaProK with (e) GGG-
 141 A and (f) GGG-B.

142

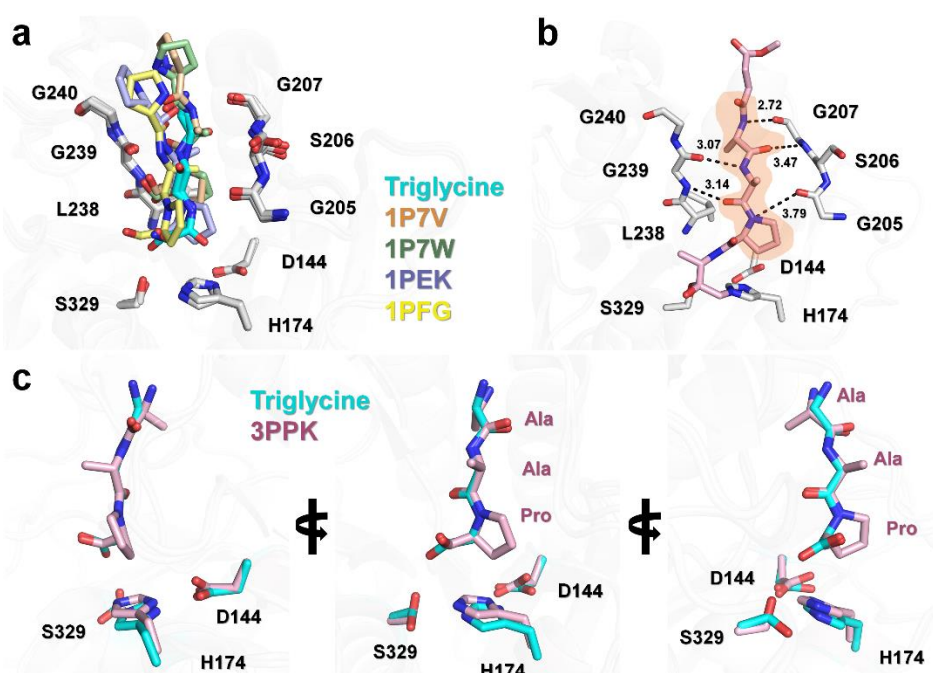
143 3.3. Structural Comparison of PaProK-triglycine complex with other ProK-inhibitor peptide

144 X-ray crystal structure confirmed that triglycine binds at the PaProK substrate recognition site
 145 in two different conformations. To confirm whether main-chain interactions between PaProK and
 146 triglycine provide information for FBDD, PaProK-triglycine was compared with a previously
 147 reported crystal structures of PaProK complexed with a peptide-based inhibitor (Figure 3 and
 148 Supplementary Figure S1). In PDB, five proteinase K structures in complex with peptide-based
 149 inhibitors (PDB code 1P7V, 1P7W, 1PEK, 1PFG and 3PRK [25-27]) were found. These structures show
 150 structural similarity to PaProK-triglycine with an RMSD of 0.192-0.437 Å. In PaProK-1P7V (Pro-Ala-
 151 Pro-Phe-Ala-Ala-Ala) and PaProK-1P7W (Pro-Ala-Pro-Phe-Ala-Ser-Ala), the heptapeptide inhibitor
 152 is located in the cleft around the active site, the substrate binding pocket (Supplementary Figure S1).
 153 The N-terminal Pro-Ala-Pro residues of these peptide inhibitors lie in the same substrate-recognition
 154 cleft as PaProK-triglycine and C-terminal residues are proximal to $\beta 5$ - $\alpha 4$ loop (Supplementary Figure
 155 S1). The peptide-inhibitors in ProK-1PEK (N-Ac-Pro-Ala-Pro-Phe-DAla-Ala-NH₂; hexapeptide
 156 inhibitor) and ProK-1PFG (N-Ac-Pro-Ala-Pro-Phe-DAla-Ala-Ala-Ala-NH₂; octapeptide inhibitor),
 157 include N-terminal modification and D-form amino acids. These structures show the cleavage forms
 158 of inhibitor. N-terminal Pro-Ala-Pro residues of 1PEK and 1PFG are placed in the substrate
 159 recognition site, and the cleaved C-terminal fragments are located in the vicinity of the His174 residue
 160 (Supplementary Figure S1). Collectively, N-terminal Pro-Ala-Pro residues of the inhibitors in all
 161 PaProK complex structures (1P7V, 1P7W, 1PEK and 1PFG) were located in the same substrate
 162 binding position between $\beta 5$ - $\alpha 4$ and $\alpha 5$ - $\beta 6$ loops, similar to that observed with triglycine. However,

163 the four Pro-Ala-Pro residues in the peptide inhibitor not only showed different backbone geometry,
 164 but also had no similarity with the backbone interaction of triglycine. The different geometry of the
 165 backbone of these peptides is considered to be determined by the C-terminal amino acid sequence of
 166 Pro-Ala-Pro or the presence of L / D form of amino acid (Figure 3a).

167 In PaProK-3PPK (methoxysuccinyl-Ala-Ala-Pro-Ala-chloromethyl ketone), peptide-inhibitor
 168 was covalently modified and showed in transition state in crystal structure (Figure 3b). In this crystal
 169 structure, the N atom of Ala281 (number in PDB of ProK3PPK), O atom of Ala281, N3 and nitrogen
 170 atom of Ala282 and O atom of Ala282 of peptide-inhibitor interact with the O atom of Gly207 (2.72
 171 Å), N atom of Gly207 (3.47 Å), the O atom of Gly239 (3.14 Å) and the N atom of Gly239 (3.07 Å),
 172 respectively. Notably, in ProK-3PPK, the Ala-Ala-Pro residues located at the substrate binding site
 173 between $\beta 5$ - $\alpha 4$ and $\alpha 5$ - $\beta 6$ loops exhibited almost identical backbone geometry to the GGG-B form of
 174 triglycine (Figure 3c).

175



176

177 **Figure 3.** Structural comparison of PaProK-triglycine complex with PaProK complexed with other
 178 peptide-based inhibitors. (a) Superimposition of PaProK-triglycine with partial sequence (Pro-Ala-
 179 Pro) from PaProK complexed with peptide-based inhibitors (PDB codes 1P7V, 1P7W, 1PEK and
 180 1PFG). (b) Inhibitor binding configuration of PaProK-3PPK. (c) Superimposition of backbone of
 181 triglycine and Pro-Ala-Ala from peptide-based inhibitor in PaProK-3PPK.

182

183 4. Discussion

184 Understanding the mechanistic and structural characteristics of substrate recognition in PPI
 185 could provide very useful insights for FBDD. To understand the mechanism underlying substrate
 186 recognition by the target protein, X-ray crystallography-based structural investigation is generally
 187 performed using peptide fragments of a substrate or similar sequence. Here, a triglycine molecule
 188 corresponding to the peptide backbone was employed to identify the substrate binding site on
 189 PaProK. Triglycine with its two configurations was correctly placed on the substrate binding site in
 190 PaProK. This approach can provide structural information on the recognition of the main chain of a
 191 peptide-recognizing protein. Further, it could provide potential information for the initial FBDD.
 192 Comparison with PaProK-peptide-based inhibitor structures revealed that one of the configurations

193 of triglycine was found to have almost the same back-bone binding configuration as the peptide
194 inhibitor in PaProK-3PPP. This indicates that the substrate recognition evidence obtained through
195 triglycine can be translated to design novel peptide inhibitors. Further, the existence of two different
196 conformation of triglycine in the substrate binding site of PaProK was confirmed. These results
197 suggest that peptide-based inhibitors can be designed with two different conformations. However,
198 this can provide information on nonspecific binding. Therefore, further studies on peptide
199 interactions are needed, which could lead to improved products. To conclude, triglycine provided
200 information on substrate recognition mechanism in protein-protein or protein-peptide interactions
201 that can be employed in FBDD.
202

203 **Author Contributions:** K.H.N. performed the experiments and wrote the manuscript.
204

205 **Funding:** This research was funded by the National Research Foundation of Korea (NRF-2017R1D1A1B03033087
206 and 2017M3A9F6029736). This work was supported by Korea UMSIT and PAL (Korea), and the Korea University
207 Grant.
208

209 **Acknowledgments:** The authors thank the staff of macromolecule crystallography beamlines at Pohang
210 Accelerator Laboratory for assistance in data collection.
211

212 **Conflicts of Interest:** The authors declare no conflict of interest.

213 References

- 214 1. Pelay-Gimeno, M.; Glas, A.; Koch, O.; Grossmann, T. N., Structure-Based Design of Inhibitors of
215 Protein-Protein Interactions: Mimicking Peptide Binding Epitopes. *Angew Chem Int Ed Engl* **2015**, *54*,
216 (31), 8896-927.
- 217 2. Milroy, L. G.; Grossmann, T. N.; Hennig, S.; Brunsveld, L.; Ottmann, C., Modulators of protein-protein
218 interactions. *Chem Rev* **2014**, *114*, (9), 4695-748.
- 219 3. Nevola, L.; Giralt, E., Modulating protein-protein interactions: the potential of peptides. *Chem Commun*
220 (*Camb*) **2015**, *51*, (16), 3302-15.
- 221 4. Stanfield, R. L.; Wilson, I. A., Protein-peptide interactions. *Curr Opin Struct Biol* **1995**, *5*, (1), 103-13.
- 222 5. Wells, J. A.; McClendon, C. L., Reaching for high-hanging fruit in drug discovery at protein-protein
223 interfaces. *Nature* **2007**, *450*, (7172), 1001-9.
- 224 6. Craik, D. J.; Fairlie, D. P.; Liras, S.; Price, D., The future of peptide-based drugs. *Chem Biol Drug Des*
225 **2013**, *81*, (1), 136-47.
- 226 7. Fosgerau, K.; Hoffmann, T., Peptide therapeutics: current status and future directions. *Drug Discov*
227 *Today* **2015**, *20*, (1), 122-8.
- 228 8. Tounge, B. A.; Parker, M. H., Designing a diverse high-quality library for crystallography-based FBDD
229 screening. *Methods Enzymol* **2011**, *493*, 3-20.
- 230 9. Murray, C. W.; Rees, D. C., The rise of fragment-based drug discovery. *Nat Chem* **2009**, *1*, (3), 187-92.
- 231 10. Carr, R. A.; Congreve, M.; Murray, C. W.; Rees, D. C., Fragment-based lead discovery: leads by design.
232 *Drug Discov Today* **2005**, *10*, (14), 987-92.
- 233 11. Ebeling, W.; Hennrich, N.; Klockow, M.; Metz, H.; Orth, H. D.; Lang, H., Proteinase K from *Tritirachium*
234 *album* Limber. *Eur J Biochem* **1974**, *47*, (1), 91-7.
- 235 12. Muller, A.; Hinrichs, W.; Wolf, W. M.; Saenger, W., Crystal structure of calcium-free proteinase K at
236 1.5-Å resolution. *J Biol Chem* **1994**, *269*, (37), 23108-11.

- 237 13. Park, S. Y.; Ha, S. C.; Kim, Y. G., The Protein Crystallography Beamlines at the Pohang Light Source II
238 *Biodesign* **2017**, 5, (1), 30-34.
- 239 14. Otwinowski, Z.; Minor, W., Processing of X-ray diffraction data collected in oscillation mode. *Methods*
240 *Enzymol* **1997**, 276, 307-26.
- 241 15. Vagin, A.; Teplyakov, A., Molecular replacement with MOLREP. *Acta Crystallogr D Biol Crystallogr* **2010**,
242 66, (Pt 1), 22-5.
- 243 16. Potterton, L.; McNicholas, S.; Krissinel, E.; Gruber, J.; Cowtan, K.; Emsley, P.; Murshudov, G. N.; Cohen,
244 S.; Perrakis, A.; Noble, M., Developments in the CCP4 molecular-graphics project. *Acta Crystallogr D*
245 *Biol Crystallogr* **2004**, 60, (Pt 12 Pt 1), 2288-94.
- 246 17. Betzel, C.; Gourinath, S.; Kumar, P.; Kaur, P.; Perbandt, M.; Eschenburg, S.; Singh, T. P., Structure of a
247 serine protease proteinase K from *Tritirachium album limber* at 0.98 Å resolution. *Biochemistry* **2001**, 40,
248 (10), 3080-8.
- 249 18. Emsley, P.; Cowtan, K., Coot: model-building tools for molecular graphics. *Acta Crystallogr D Biol*
250 *Crystallogr* **2004**, 60, (Pt 12 Pt 1), 2126-32.
- 251 19. Adams, P. D.; Afonine, P. V.; Bunkoczi, G.; Chen, V. B.; Davis, I. W.; Echols, N.; Headd, J. J.; Hung, L.
252 W.; Kapral, G. J.; Grosse-Kunstleve, R. W.; McCoy, A. J.; Moriarty, N. W.; Oeffner, R.; Read, R. J.;
253 Richardson, D. C.; Richardson, J. S.; Terwilliger, T. C.; Zwart, P. H., PHENIX: a comprehensive Python-
254 based system for macromolecular structure solution. *Acta Crystallogr D Biol Crystallogr* **2010**, 66, (Pt 2),
255 213-21.
- 256 20. Williams, C. J.; Headd, J. J.; Moriarty, N. W.; Prisant, M. G.; Videau, L. L.; Deis, L. N.; Verma, V.; Keedy,
257 D. A.; Hintze, B. J.; Chen, V. B.; Jain, S.; Lewis, S. M.; Arendall, W. B.; Snoeyink, J.; Adams, P. D.; Lovell,
258 S. C.; Richardson, J. S.; Richardson, D. C., MolProbity: More and better reference data for improved all-
259 atom structure validation. *Protein Sci* **2018**, 27, (1), 293-315.
- 260 21. Nam, K. H.; Kim, M. Y.; Kim, S. J.; Priyadarshi, A.; Kwon, S. T.; Koo, B. S.; Yoon, S. H.; Hwang, K. Y.,
261 Structural and functional analysis of a novel hormone-sensitive lipase from a metagenome library.
262 *Proteins* **2009**, 74, (4), 1036-40.
- 263 22. Nam, K. H.; Kim, M. Y.; Kim, S. J.; Priyadarshi, A.; Lee, W. H.; Hwang, K. Y., Structural and functional
264 analysis of a novel EstE5 belonging to the subfamily of hormone-sensitive lipase. *Biochem Biophys Res*
265 *Commun* **2009**, 379, (2), 553-6.
- 266 23. Nam, K. H.; Kim, S. J.; Priyadarshi, A.; Kim, H. S.; Hwang, K. Y., The crystal structure of an HSL-
267 homolog EstE5 complex with PMSF reveals a unique configuration that inhibits the nucleophile Ser144
268 in catalytic triads. *Biochem Biophys Res Commun* **2009**, 389, (2), 247-50.
- 269 24. Nam, K.-H.; Park, S.-H.; Lee, W.-H.; Hwang, K.-Y., Biochemical and Structural Analysis of Hormone-
270 sensitive Lipase Homolog EstE7: Insight into the Stabilized Dimerization of HSL-Homolog Proteins.
271 *Bulletin of the Korean Chemical Society* **2010**, 31, (9), 2627-2632.
- 272 25. Saxena, A. K.; Singh, T. P.; Peters, K.; Fittkau, S.; Betzel, C., Strategy to design peptide inhibitors:
273 structure of a complex of proteinase K with a designed octapeptide inhibitor N-Ac-Pro-Ala-Pro-Phe-
274 DAla-Ala-Ala-Ala-NH₂ at 2.5 Å resolution. *Protein Sci* **1996**, 5, (12), 2453-8.
- 275 26. Betzel, C.; Singh, T. P.; Visanji, M.; Peters, K.; Fittkau, S.; Saenger, W.; Wilson, K. S., Structure of the
276 complex of proteinase K with a substrate analogue hexapeptide inhibitor at 2.2-Å resolution. *J Biol Chem*
277 **1993**, 268, (21), 15854-8.

- 278 27. Wolf, W. M.; Bajorath, J.; Muller, A.; Raghunathan, S.; Singh, T. P.; Hinrichs, W.; Saenger, W., Inhibition
279 of proteinase K by methoxysuccinyl-Ala-Ala-Pro-Ala-chloromethyl ketone. An x-ray study at 2.2-Å
280 resolution. *J Biol Chem* **1991**, 266, (26), 17695-9.
281